

Crystal structure and melting in a cell model. II. First-order transitions and metastable states

This article has been downloaded from IOPscience. Please scroll down to see the full text article.

1971 J. Phys. A: Gen. Phys. 4 728

(<http://iopscience.iop.org/0022-3689/4/5/014>)

View [the table of contents for this issue](#), or go to the [journal homepage](#) for more

Download details:

IP Address: 171.66.16.73

The article was downloaded on 02/06/2010 at 04:35

Please note that [terms and conditions apply](#).

Crystal structure and melting in a cell model II. First-order transitions and metastable states

D. J. GATES†

Mathematics Department, Imperial College, London SW7, England

MS. received 30th December 1970

Abstract. The detailed thermodynamics of the cases of the cell model in paper I is considered. The one-dimensional systems have a first-order melting transition if the interactions extend beyond nearest-neighbour cells. The nearest-neighbour case has a second-order transition. First-order transitions also occur for a triangular lattice with nearest-neighbour interactions, a square lattice with first- and second-neighbour interactions, and others. The isotherms for the first-order transitions closely resemble those obtained numerically for a hard square lattice gas by Bellemans and Nigam. The antiferromagnetic version of the cell model on a triangular lattice has two different ordered states and two transitions. Metastable states are defined and located for both the fluid and crystalline phases, and have some surprising features.

1. Introduction

A simple model of melting which has been the subject of some recent work is the lattice gas of hard particles, which we shall call the *hard core lattice gas* (hclg). In this model the particles can move from site to site on a lattice, but are prevented from approaching each other too closely by a repulsive potential of infinite strength. For the special case where the hard core extends to nearest-neighbour sites on a square lattice, numerical analysis (Gaunt and Fisher 1965, Gaunt 1966) suggests that there is a second-order melting transition. If, however, the hard core extends to third neighbours numerical analysis (Bellemans and Nigam 1967) suggests that there is a melting transition of the first order. (The case of second neighbours is in doubt.)

Why should the second-order transition be peculiar to the near-neighbour models? This puzzling question has not yet been answered. (Furthermore, it is not known for certain that the transitions are of the suspected types since no rigorous proofs yet exist.) In this paper we show (rigorously) that precisely the same peculiarity is possessed by the cell model considered in paper I (Gates 1971a) and introduced in a previous paper (Gates 1971b to be referred to as ESCM).

In ESCM it was shown that the special case of this cell model with repulsive nearest-neighbour interactions on a cubic lattice, of any number of dimensions, has a second-order melting transition. This case is analogous to the hclg on a square or cubic lattice, both of which have a second-order transition according to Gaunt (1966). Likewise the cell model on a bcc lattice with nearest-neighbour interactions gives a second-order transition (see paper I, § 1), which again agrees with the hclg (Gaunt 1966). A case not considered by Gaunt is the plane honeycomb lattice, which for the cell model has a second-order transition (paper I, § 1). This corresponds to a hclg consisting of hard triangles, which one might expect to again have a second-order transition because the core size is small (see Bellemans and Nigam 1967).

As mentioned above, the numerical work of Bellemans and Nigam (1967) suggests that the plane square hclg with a core extending to many neighbours has a first-order

† Now at the Rockefeller University, New York, NY 10021, USA.

melting transition. We prove (in § 3) an analogous result for the class of one-dimensional systems considered in paper I, and consequently for the systems isomorphic to these systems (paper I, § 4). The latter include the triangular lattice and the square lattice with diagonal interactions (analogous to the second-neighbour hclg).

Gaunt (1966) however finds that the hclg on a triangular lattice (i.e. hard hexagonal particles) has a second-order transition, although this is not rigorously proved. The two models therefore appear to have transitions of different order in this case. One would expect this to be a rather critical case because, having only first neighbour interactions, one might suspect a second-order transition; but, because the particle size is fairly large, one might expect a first-order transition. Perhaps some more accurate work on the hclg case might be worth while, just to see how complete the agreement between the two models is.

2. Plain triangular lattice, or one-dimensional, second-neighbour lattice

In this section we examine the thermodynamics corresponding to the free energy (4.3) of paper I, for the special case

$$q(\mathbf{r}) = 0 \quad K_0 = 0$$

giving

$$\alpha = 6K_1 > 0. \tag{2.1}$$

Then, with the notation of paper I, we obtain for this free energy

$$a(\rho, T) = \text{CE}\{E^3(a^0(\rho, T) - \frac{1}{4}\alpha\rho^2) + \frac{3}{4}\alpha\rho^2\} \tag{2.2}$$

where

$$a^0(\rho, T) = kT\{\rho \lg(\Lambda^\nu\rho) - \rho\} \tag{2.3}$$

is the ideal gas free energy, Λ is the thermal wavelength, and $\nu = 1$ or 2 depending on which system we are considering. Now we use the fact that for any function $g(\rho)$ and any constants P and Q

$$E^L(g(\rho) + P\rho + Q) = E^Lg(\rho) + P\rho + Q$$

and

$$\text{CE}(g(\rho) + P\rho + Q) = \text{CE}g(\rho) + P\rho + Q. \tag{2.4}$$

The first equation follows from equation (3.2) of paper I and the second is equation (5.6) of ESCM. Substituting equation (2.3) in (2.2) and using (2.4) gives

$$a(\rho, T) = Aa_r(B\rho) + C\rho \tag{2.5}$$

where

$$a_r(\eta) \equiv \text{CE}\{E^3(\eta \lg \eta - \frac{1}{2}\eta^2) + \frac{3}{2}\eta^2\} \tag{2.6}$$

which we call the *reduced free energy*

$$A(T) \equiv \frac{2(kT)^2}{\alpha}$$

$$B(T) \equiv \frac{\alpha}{2kT}$$

and

$$C(T) \equiv kT \left\{ \lg \frac{2\Lambda^\nu kT}{\alpha} - 1 \right\}. \tag{2.7}$$

As in ESCM, these results imply that there is *no critical temperature*. The reduced

free energy $a_r(\eta)$ completely determines the thermodynamics. To study this we write

$$f(\eta) \equiv \eta \lg \eta - \frac{1}{2}\eta^2 \quad (2.8)$$

and obtain from (3.2) of paper I

$$E^3 f(\eta) = \frac{1}{3}f(\eta + \delta_1(\eta)) + \frac{1}{3}f(\eta + \delta_2(\eta)) + \frac{1}{3}f(\eta + \delta_3(\eta)) \quad (2.9)$$

where the δ minimize the right side, subject to

$$\delta_1 + \delta_2 + \delta_3 = 0. \quad (2.10)$$

The variational condition for this minimum yields

$$f'(\eta + \delta_1) = f'(\eta + \delta_2) = f'(\eta + \delta_3). \quad (2.11)$$

At this point it is more convenient to consider the chemical potential

$$\begin{aligned} \mu(\rho, T) &= \frac{\partial}{\partial \rho} a(\rho, T) \\ &= kT\mu_r(B\rho) + C \end{aligned} \quad (2.14)$$

where

$$\mu_r(\eta) \equiv \frac{\partial}{\partial \eta} a_r(\eta) \quad (2.13)$$

which we call the *reduced chemical potential*. To calculate $\mu_r(\eta)$ we use (2.6) to obtain

$$\mu_r(\eta) = \text{MC} \left\{ \frac{\partial}{\partial \eta} (E^3 f(\eta)) + 3\eta \right\} \quad (2.14)$$

where MC means 'apply the Maxwell construction (or equal area rule) with respect to η (see Lebowitz and Penrose 1966) to the expression in brackets'. Now from (2.9) and (2.11) we have

$$\begin{aligned} \theta(\eta) &\equiv \frac{\partial}{\partial \eta} (E^3 f(\eta)) = \frac{1}{3} \sum_{i=1}^3 f'(\eta + \delta_i(\eta))(1 + \delta_i'(\eta)) \\ &= f'(\eta + \delta_i(\eta)) \text{ for all } i \end{aligned} \quad (2.15)$$

since $\delta_1' + \delta_2' + \delta_3' = 0$. By plotting the function (figure 1)

$$f'(\eta) = \lg \eta - \eta + 1 \quad (2.16)$$

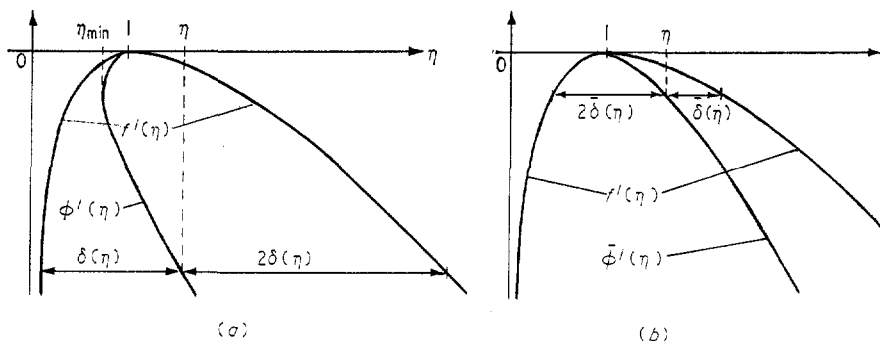


Figure 1. Illustration of the functions $\delta(\eta)$ and $\bar{\delta}(\eta)$ given in equation (2.17). Here $\eta_{\min} \simeq 0.915$.

we see that (2.11) has 3 solutions (ignoring permutations of suffices). The first, $\delta_i(\eta) = 0$ for all i and η , is trivial. The others are of the form

$$\delta_1(\eta) = \delta_2(\eta) = -\delta(\eta) \quad \delta_3(\eta) = 2\delta(\eta) \quad (2.17a)$$

$$\delta_1(\eta) = \delta_2(\eta) = \bar{\delta}(\eta) \quad \delta_3(\eta) = -2\bar{\delta}(\eta) \quad (2.17b)$$

where $\delta(\eta) \geq 0$ and $\bar{\delta}(\eta) \geq 0$. To find which of these corresponds to the minimum in (2.9) we consider the functions

$$\begin{aligned} \phi(\eta) &\equiv \frac{2}{3}f(\eta - \delta) + \frac{1}{3}f(\eta + 2\delta) \\ \bar{\phi}(\eta) &\equiv \frac{2}{3}f(\eta + \bar{\delta}) + \frac{1}{3}f(\eta - 2\bar{\delta}). \end{aligned} \quad (2.18)$$

These functions are sketched in figure 2, which shows that the minimum in (2.9)

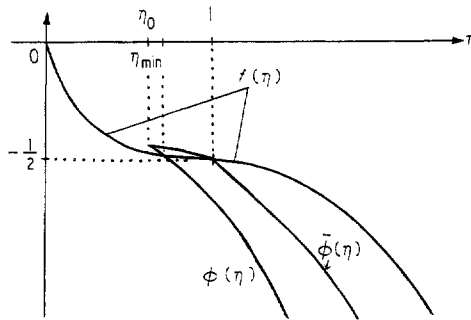


Figure 2. Illustration of the functions $\phi(\eta)$ and $\bar{\phi}(\eta)$, given by equation (2.18) showing that $\phi(\eta) < \bar{\phi}(\eta)$.

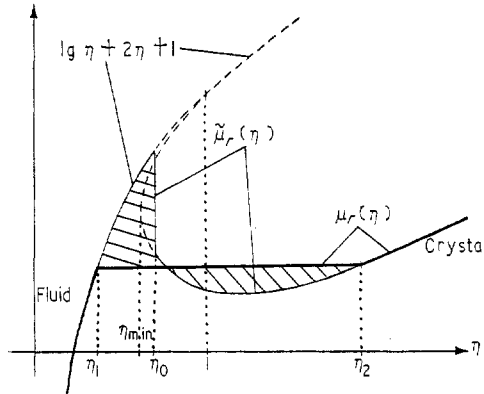


Figure 3. Sketch of the reduced chemical potential $\mu_r(\eta)$ (thick line), which gives the true chemical potential through equation (2.12). The shaded areas are equal, according to equation (2.22).

is given by

$$E^3 f(\eta) = \begin{cases} f(\eta) & \eta \leq \eta_0 \\ \phi(\eta) & \eta \geq \eta_0 \end{cases} \quad (2.19)$$

where $\eta_0 \approx 0.924$ is the value of η where the lower branch of $\phi(\eta)$ cuts $f(\eta)$. The

function $\bar{\phi}(\eta)$ never represents a minimum. We now have

$$\frac{\partial}{\partial \eta} E^3 f(\eta) = \begin{cases} f'(\eta) & \eta < \eta_0 \\ \phi'(\eta) & \eta > \eta_0 \end{cases} \quad (2.20)$$

which is discontinuous (see figures 1(a) and 3). The functions

$$\tilde{\mu}_r(\eta) \equiv \frac{\partial}{\partial \eta} E^3 f(\eta) + 3\eta \quad (2.21)$$

and from (2.14)

$$\mu_r(\eta) = MC \tilde{\mu}_r(\eta) \quad (2.22)$$

are sketched in figure 3. The curve $\mu_r(\eta)$ has a flat portion between η_1 and η_2 . From (2.12) it follows that $\mu(\rho, T)$ against ρ has a flat portion for

$$2kT\eta_1/\alpha \leq \rho \leq 2kT\eta_2/\alpha$$

which represents a *first-order phase transition*. We find that $\eta_1 \simeq 0.840$ and $\eta_2 \simeq 1.276$. If this is compared with the isotherms shown in figures 9 and 11 of Bellemans and Nigam (1967) for the first-order transition in a third-neighbour helg, a remarkable similarity will be found. The author is unable to explain this.

The canonical pressure $\pi(\rho, T)$ can be found as in ESCM. As there, we obtain

$$\pi(\rho, T) = \rho kT + \frac{1}{2}\alpha\rho^2 \text{ for } \rho \leq 2kT\eta_1/\alpha \quad (2.23)$$

so that at the transition density

$$\pi = \frac{2\eta_1(1 + \eta_1)k^2}{\alpha} T^2. \quad (2.24)$$

Thus the phase diagram is a parabola as in the nearest-neighbour case (equation (5.47) of ESCM). Isotherms of $\pi(\rho, T)$ are sketched in figure 4.

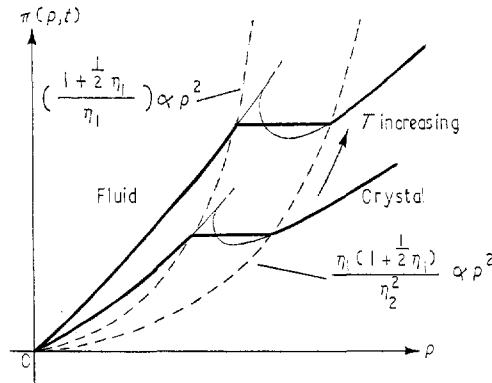


Figure 4. Two typical isotherms of the pressure $\pi(\rho, T)$ (thick lines), showing their continuations (thin lines) and the boundary of the two-phase region (broken line).

The crystal state ($\eta > \eta_2$) is here given by (2.17a); that is, the system has a local density $n^*(y)$ with two values

$$\rho_{\pm}(\rho, T) = \frac{2kT}{\alpha} \eta_{\pm} \left(\frac{\alpha\rho}{2kT} \right)$$

where

$$\begin{aligned} \eta_+(\eta) &\equiv \eta + 2\delta(\eta) \\ \eta_-(\eta) &\equiv \eta - \delta(\eta). \end{aligned} \tag{2.25}$$

The densities are, according to § 4 of paper I, arranged as shown in figure 5. The

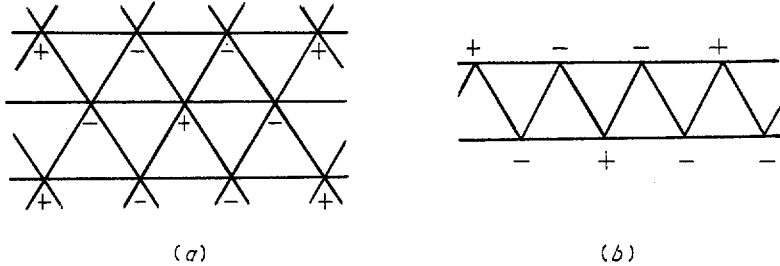


Figure 5. Arrangement of the local densities ρ_+ and ρ_- for the case (2.1) on (a) the triangular lattice, and (b) the solvable one-dimensional lattice with first- and second-neighbour interactions.

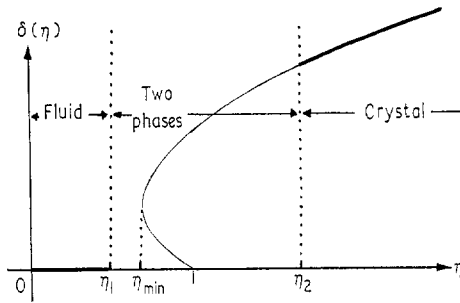


Figure 6. Sketch of the function $\delta(\eta)$, given by equation (2.26) for $\eta > \eta_2$.

function $\delta(\eta)$ which determines ρ_+ and ρ_- is sketched in figure 6. From (2.11) and (2.17a) the complete function for the crystal phase is given implicitly by the equation

$$f'(\eta + 2\delta) = f'(\eta - \delta)$$

which reduces to

$$\eta = \delta + \frac{3\delta}{(e^{3\delta} - 1)} \tag{2.26}$$

which we use in § 6. Only the part $\eta > \eta_2$ has any significance, while $\delta = 0$ for fluid states ($\eta < \eta_1$).

3. A class of one-dimensional cases

In this section we consider briefly the thermodynamics of the one-dimensional model with L -neighbour interactions introduced in paper I, § 3. We deal with the special case

$$q(\mathbf{r}) = 0 \quad \text{and} \quad K_0 = 0 \tag{3.1}$$

for which the free energy (3.3) of paper I reduces to

$$a(\rho, T) = CE\{E^L(a^0(\rho, T) - \frac{1}{2}Lb\rho^2) + \frac{1}{2}L^2b\rho^2\} \tag{3.2}$$

where a^0 is given by (2.3). Applying (2.4) we now obtain

$$a(\rho, T) = Aa_r(B\rho) + C\rho \tag{3.3}$$

where

$$a_r(\eta) \equiv \text{CE}\{E^L(\eta \lg \eta - \frac{1}{2}\eta^2) + \frac{1}{2}L\eta^2\} \tag{3.4}$$

$$A(T) \equiv \frac{(kT)^2}{bL}$$

$$B(T) \equiv \frac{bL}{kT}$$

and

$$C(T) \equiv kT \left(\lg \frac{\Lambda^v kT}{Lb} - 1 \right). \tag{3.5}$$

Now we proceed essentially as before. The function $E^L f(\eta)$ is obtained by a construction like that in figure 1. Here the appropriate construction is the locus of the points one L th of the way along the horizontal chords of $f(\eta)$. Again the reduced chemical potential $\mu_r(\eta)$ has a form like that shown in figure 3, so that the transition is again first-order. The coexistence curve is again a parabola. Now the crystal state has a density $n^*(y)$ of the form

$$\begin{aligned} n^*(y) &= \rho_+ & y &= 1 \\ &= \rho_- & y &= 2, \dots L \end{aligned} \tag{3.6}$$

and has period L .

The lattices isomorphic to cases of the above system have, by definition, the same thermodynamics. They also have a local density with two values ρ_+ and ρ_- (under conditions (3.1)). For example, the plane square lattice with diagonal bonds (equation (4.5) of paper I), which is isomorphic to the $L = 4$ case above, has the crystal structure shown in figure 7.

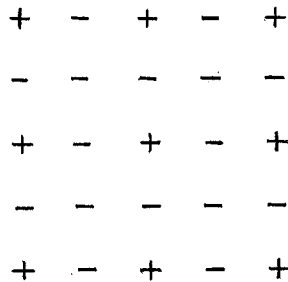


Figure 7. Arrangement of densities ρ_+ and ρ_- on the square lattice with first- and second-neighbour interactions for the case (3.1).

The two-phase region again corresponds to an interval $\eta_1 < \eta < \eta_2$. From (3.3) and (3.5) this in turn corresponds to an interval $kT\eta_1/bL < \rho < kT\eta_2/bL$, that is, to

$$\frac{(L-1)kT\eta_1}{\alpha} < \rho < \frac{(L-1)kT\eta_2}{\alpha}. \tag{3.7}$$

Thus, if we keep α fixed (i.e. the 'area' under $K(s)$) and let $b \rightarrow 0$ and $L \rightarrow \infty$, the

transition occurs at higher and higher densities. In a way, this explains why the continuum model (equation (5.2) of paper I) shows no phase transition and no crystal state.

4. Antiferromagnet on triangular and one-dimensional second-neighbour lattices

In ESCM, section 7 a magnetic version of the cell model, in which the cells contain spins instead of particles, was considered. It was shown that the nearest-neighbour version of the model on a ν -dimensional cubic lattice, with antiferromagnetic interactions ($K_1 > 0$), results in precisely the Néel-van Vleck (or mean field) theory of antiferromagnetism. In the present section we consider the same model on the two isomorphic lattices: the plane triangular lattice and the one-dimensional, second-neighbour lattice (paper I, § 4).

On these lattices the free energy per spin $a(\rho, T)$, for an average magnetization per spin ρ (where $-1 < \rho < 1$), is given as in (2.2) by

$$a(\rho, T) = CE\{E^3(a^0(\rho, T) - \frac{1}{4}\alpha\rho^2) + \frac{3}{4}\alpha\rho^2\} \tag{4.1}$$

where here

$$a^0(\rho, T) = kT\left\{\left(\frac{1+\rho}{2}\right) \lg\left(\frac{1+\rho}{2}\right) + \left(\frac{1-\rho}{2}\right) \lg\left(\frac{1-\rho}{2}\right)\right\} \tag{4.2}$$

which is the free energy per spin of an ideal magnet, and $\alpha > 0$. The simplification leading to (2.5) does not apply here, so that the behaviour of the system is more complicated. However, the analysis following (2.8) can essentially be applied to (4.1). Here we choose, for fixed α and T

$$f(\rho) \equiv a^0(\rho, T) - \frac{1}{4}\alpha\rho^2. \tag{4.3}$$

The function $f'(\rho)$ is sketched in figure 8. Now equation (2.11) is replaced by

$$f'(\rho + \delta_1) = f'(\rho + \delta_2) = f'(\rho + \delta_3). \tag{4.4}$$

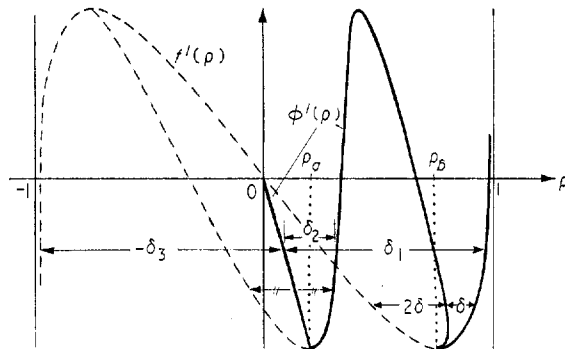


Figure 8. Sketch of the function $\phi'(\rho)$ (for $\rho > 0$), which gives the magnetic field $H(\rho)$ through equation (4.7), for the antiferromagnet on a triangular lattice. The lines marked with a double stroke have equal length (cf. figure 1).

For $|\rho| > \rho_a$ (see figure 8), this has only solutions of the form (2.17). As there, the solution corresponding to the minimum (which gives E^{3f}) is of the form (2.17a), i.e.

$$\delta_1(\rho) = \delta_2(\rho) = -\delta(\rho) \quad \delta_3(\rho) = 2\delta(\rho). \tag{4.5}$$

For $|\rho| < \rho_a$, on the other hand, there is a further solution with all the δ_i different, and this corresponds to the minimum. The graphical construction which gives all the δ is shown in figure 8. The magnetic field $H(\rho)$ as a function of magnetization ρ (for fixed T)

$$H(\rho) = \frac{\partial a(\rho)}{\partial \rho} \quad (4.6)$$

is given by

$$H(\rho) = \text{MC}\{\phi'(\rho) + \frac{3}{2}\alpha\rho\} \quad (4.7)$$

where $\phi'(\rho)$ is shown in figure 8, and MC means, as before, the Maxwell construction. A typical (low temperature) isotherm of $H(\rho)$ is sketched in figure 9. As indicated

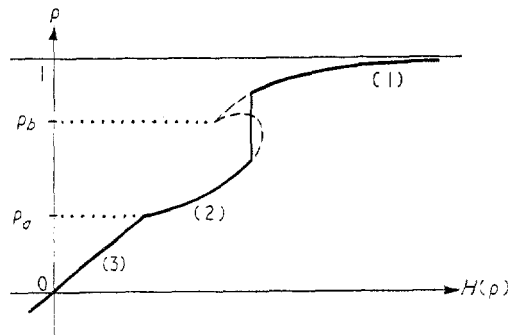


Figure 9. The field H against magnetization ρ on the triangular-lattice antiferromagnet, showing the three phases and two transitions.

there are three states and two transitions. State (1) (high ρ and H) has a uniform local magnetization $n^*(\mathbf{y}) = \rho$. State (2) (medium ρ and H) has a local magnetization with two values ρ_+ and ρ_- arranged as in figure 4. State (3) (low ρ and H) has a local magnetization with three values ρ_1, ρ_2, ρ_3 arranged as in figure 2 of paper I. The transition (1) \rightarrow (2) appears from figure 8 to be second order, and the transition (2) \rightarrow (3) first order, but to establish this properly would require a detailed analysis.

From figure 8 it is apparent that both transitions have the same Néel temperature; that is, the temperature above which the ordered state does not exist for any ρ . This is given by $kT_N = \frac{1}{2}\alpha$. The H - T phase diagram is sketched in figure 10.

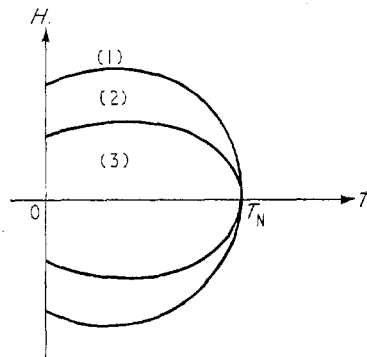


Figure 10. The phase diagram for the triangular-lattice antiferromagnet, showing the three phases.

The present model does not behave in the same way as the antiferromagnetic Ising model on a triangular lattice (Burley 1965, Stevenson 1970). The latter has only a single transition. This is probably due to the fact that the local magnetization (i.e. spin) on each lattice site can have only two values, +1 and -1, which does not permit the symmetric ordered states attained by the cell model. On the other hand, the classical, continuous-spin, Heisenberg model (see Domb 1970) does allow such ordered states, so that, possibly, it also has two transitions.

The particle system on the same lattice has a similar behaviour if the short-range potential $q(\mathbf{r})$ has a hard core (unlike § 2 where $q = 0$). Roughly speaking this is because, for such a q , the free energy $a^0(\rho, T)$ has an increasing second ρ derivative for large ρ , as does (4.2).

5. Metastable states: nearest-neighbour case

The chemical potential $\mu(\rho, T)$ of the nearest-neighbour cell model considered in ESCM was given there by

$$\mu(\rho, T) = kT\mu_r\left(\frac{\rho\alpha}{kT}\right) + C(T) \tag{5.1}$$

where $\mu_r(\eta)$ has the form shown in figure 11, $\alpha = 2\nu K(1) > 0$ and C is given by (2.7). This system has a fluid state for $\eta < 1$ i.e. $\rho < kT/\alpha$, and a crystal state for $\eta > 1$, i.e. $\rho > kT/\alpha$, with a second-order melting transition at $\rho = kT/\alpha$.

From ESCM it follows that the crystalline part $\eta > 1$ of the function $\mu_r(\eta)$ cannot be continued analytically to $\eta < 1$: it has in fact a singularity of the form $(\eta - 1)^{3/2}$ at $\eta = 1$. On the other hand, the fluid part $\eta < 1$ of the function has an obvious analytic continuation to all $\eta > 1$, shown by the broken line in figure 11.

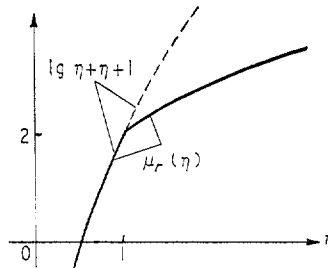


Figure 11. Stable (continuous line) and unstable (broken line) states for the ν -dimensional cubic lattice with first-neighbour interactions. There are no metastable states.

The question therefore arises: does this broken line, or any part of it, represent a metastable fluid state? To answer this question we shall adopt the following definition of the metastable free energy:

Definition. If, for $n \in \mathcal{C}(\rho)$, the functional $G(n, T)$ has a local minimum $n^*(\mathbf{y}, \rho, T)$ which is not an absolute minimum, then the function

$$a_m(\rho, T) \equiv G(n^*, T) \tag{5.2}$$

is called the metastable free energy.

The 'local minimum' here is in the coordinate space of the variables $n(\mathbf{y}_1), n(\mathbf{y}_2), \dots$, where $\mathbf{y}_1, \mathbf{y}_2, \dots$ are fixed points which make up a unit cell of n . Notice that

this definition admits both fluid ($n^* = \rho$) and crystalline metastable states. To justify the definition properly one would have to show that it followed from a suitable kinetic theory of metastability (see Lebowitz and Penrose 1971, in this connection). We shall not attempt this here. We note however that similar definitions have been used by other authors (Langer 1968). Also, we will show that it yields precisely the usual metastable states in the case of the generalized van der Waals equation (see paper I, equation (2.7))

$$a(\rho, T) = CE(a^0(\rho, T) + \frac{1}{2}\alpha\rho^2). \tag{5.3}$$

To find the general condition that n^* be a local minimum of $G(n)$, we expand $G(n)$ about n^* as a Taylor series in $h(\mathbf{y}) \equiv n(\mathbf{y}) - n^*(\mathbf{y})$ for some $n \in \mathcal{C}(\rho)$. This gives

$$G(n) = G(n^*) + Q(h) + O(h^3) \tag{5.4}$$

where Q is the quadratic form

$$Q(h) \equiv \lim_{|D| \rightarrow \infty} \frac{1}{|D|} \sum_{\mathbf{y} \in D} \{a_2^0[n^*(\mathbf{y})]h(\mathbf{y})^2 + h(\mathbf{y}) \sum_{\mathbf{y}' \in L(1)} K(\mathbf{y} - \mathbf{y}')h(\mathbf{y}')\} \tag{5.5}$$

and

$$a_2^0(\rho) \equiv \frac{\partial^2 a^0(\rho)}{\partial \rho^2}.$$

Here $L(1)$ is the lattice and D is a suitable subset of it, containing $|D|$ points (see paper I and ESCM). There is no term linear in h in (5.4) because n^* is a stationary point of G . *Therefore, a condition that n^* be a local minimum of G is that the quadratic form $Q(h)$ be positive-definite for any periodic $h(\mathbf{y})$.*

For the special case of fluid metastable states ($n^* = \rho$), (5.5) reduces to

$$Q(h) = \sum_{\mathbf{p} \in \Gamma'} (a_2^0(\rho) + \hat{K}(\mathbf{p})) |h(\mathbf{p})|^2 \tag{5.6}$$

where

$$\hat{h}(\mathbf{p}) \equiv \frac{1}{|\Gamma|} \sum_{\mathbf{y} \in \Gamma} h(\mathbf{y}) \exp(2\pi i \mathbf{p} \cdot \mathbf{y})$$

and

$$\hat{K}(\mathbf{p}) \equiv \sum_{\mathbf{s} \in L(1)} K(\mathbf{s}) \exp(2\pi i \mathbf{p} \cdot \mathbf{y}). \tag{5.7}$$

Here Γ is the unit cell of $h(\mathbf{y})$, and Γ' is the reciprocal lattice corresponding to Γ . It follows from (5.6) that Q is positive-definite if and only if

$$a_2^0(\rho) + \hat{K}_{\min} > 0 \tag{5.8}$$

where \hat{K}_{\min} is the minimum of $\hat{K}(\mathbf{p})$.

Now returning to the van der Waals case (5.3), we have here (see Gates and Penrose 1970), $\hat{K}_{\min} = \alpha$. Hence from (5.2, 4, 6 and 8) it follows that there is a metastable free energy.

$$a_m(\rho, T) = a^0(\rho, T) + \frac{1}{2}\alpha\rho^2 \tag{5.9}$$

for values of ρ and T where $a^0 + \frac{1}{2}\alpha\rho^2$ is both locally convex (i.e. $a_2^0 + \alpha > 0$) and differs from its convex envelope. This is precisely the usual result.

Next we return to the nearest-neighbour case introduced at the beginning of this section. In this case we have $\hat{K}_{\min} = -2\nu K(1) = -\alpha$ and $a_2^0(\rho) = kT/\rho$, so that (5.8) reduces to $\rho < kT/\alpha$. But this is just the stable fluid state ($\eta < 1$) of the system (figure 11). Hence the system has *no metastable states*. The analytic continuation of the stable fluid state, represented by the broken line in figure 11, is unstable.

6. Metastable states: the triangular lattices

The two isomorphous systems discussed in § 2 have more interesting metastable states. Here the chemical potential is given by (2.12–14) where $\mu_r(\eta)$, the reduced chemical potential is shown in figure 3. The fluid isotherm ($\eta < \eta_1$) has an analytic continuation to all $\eta > \eta_1$, while the crystal isotherm ($\eta > \eta_2$) has an analytic continuation with a branch point at η_{\min} . We shall find that a part, but not all, of each of these continuations represents a metastable state.

The fluid metastable states are given by (5.8). Here we have

$$\hat{K}_{\min} = -3K_1 = -\frac{1}{2}\alpha$$

and $a_2^0 = kT/\rho$, so that (5.8) reduces to $\rho < 2kT/\alpha$, that is, $\eta < 1$ in figure 12.

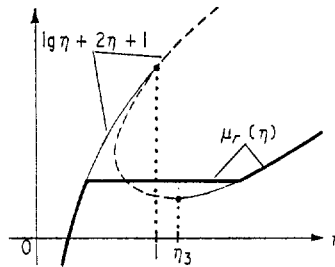


Figure 12. Stable (thick line), metastable (thin line) and unstable (broken line) states for the triangular lattice.

Consequently, we have a metastable fluid state for $\eta_1 < \eta < 1$, that is, for

$$2kT\eta_1/\alpha < \rho < 2kT/\alpha.$$

To find the metastable crystalline states we must find where the quadratic form Q is positive-definite. In the present case (5.5) reduces to (with $b \equiv K_1$)

$$Q(h) = \lim_{D \rightarrow \infty} \frac{1}{D} \sum_{y=1}^D [a_2^0 \{n^*(y)\} h(y)^2 + 4bh(y)h(y+1) + 2bh(y)h(y+2)] \quad (6.1)$$

where $n^*(y)$ is given by (2.25) and figure 5. Using the (arbitrary) periodicity of $h(y)$, this further reduces to

$$Q(h) = \lim_{M \rightarrow \infty} \frac{1}{3M} \sum_{j=1}^M [a_+ h(3j-2)^2 + a_- h(3j-1)^2 + a_- h(3j)^2 + 4b\{h(3j-2)h(3j-1) + h(3j-1)h(3j) + h(3j)h(3j+1)\} + 2b\{h(3j-2)h(3j) + h(3j-1)h(3j+1) + h(3j)h(3j+2)\}] \quad (6.2)$$

where

$$a_{\pm} \equiv a_2^0(\rho_{\pm}). \quad (6.3)$$

Because of the periodicity of $h(y)$, we can replace the term $h(3j-2)h(3j-1)$ by half the sum of itself and $h(3j+1)h(3j+2)$. Regrouping the terms then gives

$$Q(h) = \lim_{M \rightarrow \infty} \frac{1}{9M} \sum_{j=1}^M [R\{h(3j-2), h(3j-1), h(3j)\} + R\{h(3j+1), h(3j-1), h(3j)\} + R\{h(3j+1), h(3j+2), h(3j)\}] \quad (6.4)$$

where

$$R(x_1, x_2, x_3) \equiv a_+ x_1^2 + a_- (x_2^2 + x_3^2) + 6b(x_1 x_2 + x_2 x_3 + x_3 x_1) = \mathbf{x} \cdot A \cdot \mathbf{x} \quad (6.5)$$

where, in turn, $\mathbf{x} \equiv (x_1, x_2, x_3)$ and

$$A \equiv \begin{pmatrix} a_+ & 3b & 3b \\ 3b & a_- & 3b \\ 3b & 3b & a_- \end{pmatrix}. \quad (6.6)$$

The condition that Q be positive-definite therefore reduces to the condition that A be a positive-definite matrix. The latter is true if and only if every principal-minor determinant of A is positive, which requires that

$$a_- > 3b \quad (6.7)$$

$$a_+ a_- > (3b)^2 \quad (6.8)$$

$$a_+ a_-^2 - (3b)^2(a_+ + 2a_-) + 2(3b)^3 > 0. \quad (6.9)$$

Condition (6.7) reduces to $n_- < 1$. But from (2.26)

$$\eta_- = \frac{3\delta}{e^{3\delta} - 1} < 1 \text{ for all } \delta$$

(since $e^x - 1 > x$ for all x), so that (6.7) is satisfied along the entire analytic continuation of the crystal isotherm, that is, (6.7) makes no restrictions.

The second condition (6.8) reduces to $\eta_+ \eta_- < 1$. But again from (2.26)

$$\eta_+ \eta_- = \left(\frac{3\delta/2}{\sinh(3\delta/2)} \right)^2 < 1 \text{ for all } \delta \quad (6.10)$$

so that (6.8) also makes no restriction.

The third condition (6.9) reduces to

$$\frac{1}{\eta_+ \eta_-^2} - \frac{1}{\eta_+} - \frac{2}{\eta_-} + 2 > 0$$

which further reduces to

$$(1 + \eta_- - 2\eta_+ \eta_-)(1 - \eta_-) > 0.$$

Since $\eta_- < 1$, as we have just shown, this becomes

$$1 + \eta_- - 2\eta_+ \eta_- > 0. \quad (6.11)$$

To find when this holds we use (2.26) and obtain

$$1 + \eta_- - 2\eta_+ \eta_- = f(3\delta)$$

where

$$f(x) \equiv 1 + x(e^x - 1)^{-1} - 2x^2 e^x (e^x - 1)^{-2}. \quad (6.12)$$

By plotting $f(x)$ for $x \geq 0$ we find that $f(x) \leq 0$ for $x \leq x_0$ where $x_0 \simeq 2.48$. Hence (6.9) holds for $\delta > \frac{1}{3}x_0 \simeq 0.83$, which from (2.26) corresponds to

$$\eta > \eta_3 \text{ where } \eta_3 \simeq 1.06. \quad (6.13)$$

This means that the metastable crystalline states occur only in the interval (see

figure 12)

$$\eta_3 < \eta < \eta_2. \tag{6.14}$$

It turns out, as we now show, that η_3 coincides with the turning point of the continuation $\tilde{\mu}_r(\eta)$ of the crystal isotherm. To show this we use (2.21, 15, 16, and 17a) to obtain

$$\tilde{\mu}_r'(\eta) = \theta'(\eta) + 3$$

where

$$\begin{aligned} \theta(\eta) &= \lg \eta_+ - \eta_+ + 1 = \lg \eta_- - \eta_- + 1 \\ &= \frac{1}{3} \lg(\eta_+ \eta_-^2) - \eta + 1 \end{aligned} \tag{6.15}$$

since

$$\frac{1}{3}(\eta_+ + 2\eta_-) = \eta.$$

It follows from (2.25) that

$$\tilde{\mu}_r'(\eta) = \frac{\eta_- + 2\eta_+ + 6\eta_+ \eta_- + 2(\eta_- - \eta_+) \delta'(\eta)}{3\eta_+ \eta_-}. \tag{6.16}$$

But from (2.25 and 26) we have

$$\delta'(\eta) = (\eta_+ - \eta_-) / (\eta_+ + 2\eta_- - 3\eta_+ \eta_-) \tag{6.17}$$

which on substitution in (6.16) and simplification gives

$$\tilde{\mu}_r'(\eta) = \frac{1 + \eta_- - 2\eta_+ \eta_-}{\eta - \eta_+ \eta_-}. \tag{6.18}$$

Now $\eta > \eta_3$ implies $\eta > 1$, which with (6.10) gives $\eta - \eta_+ \eta_- > 0$, while $\eta - \eta_+ \eta_-$ is also clearly finite. The numerator in (6.18) is, as just shown, positive for $\eta > \eta_3$ and zero at η_3 . Hence $\tilde{\mu}_r(\eta)$ has its turning point at η_3 , which is what we wished to prove (see figure 12).

Various points about the above metastable states are of interest:

(i) As in the van der Waals equation, these states do not extend outside the two-phase region $\eta_1 < \eta < \eta_2$. Is this true of metastable states in general?

(ii) The metastable states, as in the van der Waals equation, do not meet: there is a small interval $1 < \eta < \eta_3$ where there is no such state. Is this true of metastable states in general?

(iii) All the metastable isotherms have positive gradient, that is, are thermodynamically stable. Is this true in general? It is certainly true for all cases of the present model (and of the continuum model: Gates and Penrose 1969, 1970), because from (5.2, 5.4 and 5.5) we have

$$\frac{\partial^2 a_m(\rho, T)}{\partial \rho^2} = Q \frac{\partial n^*}{\partial \rho} \tag{6.19}$$

which is positive when Q is positive-definite, that is, in all metastable states (an argument due to O. Penrose).

(iv) Unlike the van der Waals equation, not all of the continuations of the states with positive gradient are metastable (i.e. the fluid continuation for $\eta > 1$ and the upper branch of the crystal continuation). Do unstable states such as these differ thermodynamically from unstable states of negative gradient: for example, are they less unstable in some sense?

(v) The crystal metastable state extends (as in the van der Waals equation) up to a turning point. Does this always happen when there is such a turning point?

7. Discussion

We have shown that for a variety of lattices the cell model has a first-order melting transition, unlike the lattices mentioned in § 1 which have a second-order melting transition. There is a close similarity, as far as order of transition is concerned, between this model and the hclg. The common feature is that short-range interactions (i.e. small particles) result in second-order transitions, while longer-range interactions (i.e. larger particles) result in first-order transitions. Cases where they possibly differ are the triangular lattice (Gaunt 1966) and the second-neighbour hard-square case (Bellemans and Nigam 1967, Chestnut and Ree 1967), which suggests that a more accurate analysis of the hclg cases may be worth while. It might also be helpful to study the pseudo-hard-squares models of Fisher (1963) and Baxter (1970) on a triangular lattice.

The isotherms, and their continuations, for the first order melting transitions (see figures 3 and 12 for the triangular case) show a remarkable similarity to those obtained by Bellemans and Nigam (1967) for a hard-square lattice gas. Perhaps other models (for example, hard discs) have isotherms of a similar form. If so, why?

Many extensions of the present work are possible. One could study the anti-ferromagnet on a triangular lattice (§ 4) in more detail, and determine rigorously the nature of the two transitions. One might also look for experimental evidence of such transitions. The antiferromagnetic version of the one-dimensional cases of § 3 (and the related two- and three-dimensional cases) has a large number of transitions between different ordered states, and these might be worth studying. Also, the questions about metastable states at the end of § 6 present many opportunities for further work.

The correlation functions for the triangular lattices can be dealt with as in ESCM. The short-range distribution function \bar{n}_k^S considered in ESCM shows no crystalline order, but the long-range distribution function \bar{n}_k^L does, just as in ESCM. Both of these functions have a two-phase form (see equation (13) of Gates 1970) in the two-phase region. The weighted Ursell function \bar{u}_2^W considered in ESCM was shown there to have the Ornstein-Zernike form for both crystalline and fluid states, and to become long-range as these states approached the second-order transition point. For the triangular lattice it turns out that \bar{u}_2^W becomes long-range *not* at the transition points $\eta = \eta_1$ and η_2 (see figure 12), but at the points $\eta = 1$ and η_3 where the metastable isotherms end, that is, become unstable. This is just what happens in the van der Waals equation (equation (18) of Gates 1970). It seems therefore that in general this kind of long-range order occurs only when a system becomes strictly unstable.

Acknowledgments

I am grateful to D. S. Gaunt and O. Penrose for helpful advice, and to 'The Royal Commission for the Exhibition of 1851' for financial support.

Note added in proof. The existence of a phase transition in a hard core lattice gas has been given recently by Dobrushin, R. L., 1968, *Theor. Prob. Applic.*, **13**, 201-14, and 1968, *Funct. Anal. Applic.*, **2**, 31-41.

References

- BAXTER, R. J., 1970, *J. math. Phys.*, **11**, 3116-24.
 BELLEMANS, A., and NIGAM, R. K., 1967, *J. chem. Phys.*, **46**, 2922-35.
 BURLEY, D. M., 1965, *Proc. Phys. Soc.*, **85**, 1163-70.
 CHESTNUT, D. A., and REE, F. H., 1967, *Phys. Rev. Lett.*, **18**, 5-8.
 DOMB, C., 1970, *Adv. Phys.*, **19**, 339-70.

- FISHER, M. E., 1963, *J. math. Phys.*, **4**, 278–86.
GATES, D. J., 1970, *J. Phys. A: Gen. Phys.*, **3**, L11.
— 1971a, *J. Phys. A: Gen. Phys.*, **4**, 717–27.
— 1971b, *J. math. Phys.*, **12**, 766–78.
GATES, D. J., and PENROSE, O., 1969, *Commun. math. Phys.*, **15**, 255–76.
— 1970, *Commun. math. Phys.*, **17**, 194–209.
GAUNT, D. S., 1966, *J. chem. Phys.*, **46**, 3237–59.
GAUNT, D. S., and FISHER, M. E., 1965, *J. chem. Phys.*, **43**, 2840–63.
LANGER, J. S., 1968, *Phys. Rev. Lett.*, **21**, 973–6.
LEBOWITZ, J. L., and PENROSE, O., 1966, *J. math. Phys.*, **7**, 98–113.
— 1971, *J. Stat. Mech.*, in the press.
STEVENSON, J., 1970, *J. math. Phys.*, **1**, 420–31, and earlier work referred to therein.